Molecular Dynamics Simulations of Indolicidin Association with Model Lipid Bilayers

Jenny C. Y. Hsu and Christopher M. Yip
Department of Biochemistry, Terrence Donnelly Centre for Cellular and Biomolecular Research, University of Toronto, Toronto, Canada

ABSTRACT Identifying the mechanisms responsible for the interaction of peptides with cell membranes is critical to the design of new antimicrobial peptides and membrane transporters. We report here the results of a computational simulation of the interaction of the 13-residue peptide indolicidin with single-phase lipid bilayers of dioleoylphosphatidylcholine, distearoylphosphatidylcholine, dioleoylphosphatidylglycerol, and distearoylphosphatidylglycerol. Ensemble analysis of the membrane-bound peptide revealed that, in contrast to the extended, linear backbone structure reported for indolicidin in sodium dodecyl sulphate detergent micelles, the peptide adopts a boat-shaped conformation in both phosphatidylglycerol and phosphatidylcholine lipid bilayers, similar to that reported for dodecylphosphocholine micelles. In agreement with fluorescence and NMR experiments, simulations confirmed that the peptide localizes in the membrane interface, with the distance between phosphate headgroups of each leaflet being reduced in the presence of indolicidin. These data, along with a concomitant decrease in lipid order parameters for the upper-tail region, suggest that indolicidin binding results in membrane thinning, consistent with recent in situ atomic force microscopy studies.

Received for publication 3 March 2007 and in final form 3 April 2007.

Address reprint requests and inquiries to Christopher M. Yip, Tel.: 416-978-7853; Fax: 416-978-4317;
E-mail: christopher.yip@utoronto.ca.

Derived from bovine neutrophils, indolicidin is a potent antimicrobial agent comprised of only 13 amino acid residues (ILWPKWPWWPWRR-NH2). This short peptide is effective against a broad spectrum of organisms, including bacteria, fungi, protozoa, HIV-1, and T-lymphocytes (1). Like most other cationic antimicrobial peptides (AMPs), indolicidin has a +4 charge at physiological pH; however it does not adopt the α-helical or β-structure conformations seen in other AMPs. Rather, it has been shown that indolicidin adopts a disordered conformation in solution and a membrane-interacting structure containing coils and turns (2–5).

Most AMPs are believed to act by disrupting the membrane. Indolicidin's mode of action differs in that it does not induce cell lysis upon binding (6). It has been suggested that indolicidin inhibits DNA and RNA synthesis after translocating into the cell through defects that it creates in the membrane (2,6). We recently demonstrated by correlated atomic force microscopy (AFM)-confocal imaging that association of indolicidin with phase-segregated, supported planar bilayers rather than initiating pore formation, in fact causes membrane thinning (7).

To explore how indolicidin exerts its action, and to complement our experimental studies, we initiated a molecular dynamics (MD) study of indolicidin-membrane interactions using GROMACS (8). Recently, Khandelia and Kaznessis used MD approaches to examine indolicidin association in dodecylphosphocholine (DPC) and sodium dodecyl sulphate (SDS) micelles wherein they found good agreement with experimental NMR data (9). For our simulations, we computationally generated lipid bilayers similar to those used in our previous study (7), specifically dioleoylphosphatidylcholine (DOPC) (fluid-phase zwitterionic), distearoylphosphatidylcholine (DSPC) (gel-phase zwitterionic), dioleoylphosphatidylglycerol (DOPG) (fluid-phase anionic), and distearoylphosphatidylglycerol (DSPG) (gel-phase anionic). Simulations were performed on indolicidin (PDB code, 1g89) using periodic boundary conditions and a solvated single-phase 128-molecule lipid bilayer. To remove bias and provide greater statistical sampling, three peptide conformations were randomly selected after an equilibration phase of 5 ns in water. As opposed to the micelle simulations in Khandelia and Kaznessis (9) where the peptide was inserted within a micelle, in our simulations, the peptide was placed 7 Å above the bilayer in free solution so that we could examine the early stages of membrane association. All simulations were conducted over a 50-ns time period, with ensemble calculations performed on the last 20 ns of the trajectories.

Our data revealed that indolicidin partitioned into the membrane-solution interfacial region, in agreement with tryptophan fluorescence quenching experiments, spin-label lipid probe studies, and previous MD simulations of indolicidin-micelle interactions (4,9,10). Consistent with a greater electrostatic attraction between the cationic peptide and anionic lipid headgroups, our simulations revealed that indolicidin-bilayer association was fastest for the DOPG bilayers, followed by DSPG, DSPC, and DOPC cases, respectively. From a randomly structured form in solution, indolicidin adopted a range of conformations when membrane bound (Fig. 1) with Define Secondary Structure of Proteins (DSSP) analysis suggesting the existence of a bend at P3-W4 and a coil at W9-W11. The conformation of the anionic bilayer-bound indolicidin

doi: 10.1529/biophysj.107.108050

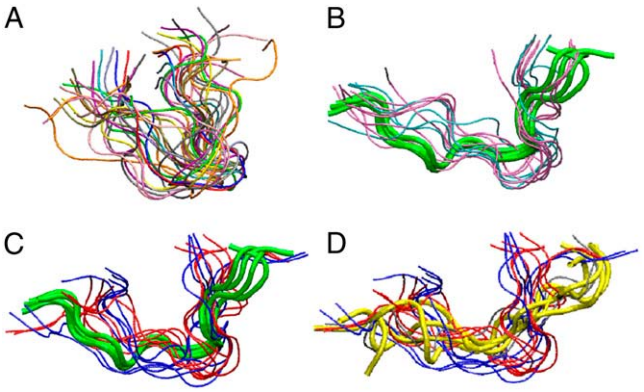

FIGURE 1 Equilibrium conformations, generated by clustering the last 20-ns trajectories of indolicidin in (*A*) water; (*B*) zwitterionic lipid bilayers (DOPC, *pink*; DSPC, *cyan*); (*C*) anionic lipid bilayers (DOPG, *red*; DSPG, *blue*). Green tubes show NMR structure of indolicidin in DPC micelles (1g89.pdb). (*D*) The same set of equilibrium conformations of indolicidin in contact with anionic lipids as in panel *C*. Yellow tubes show conformation of indolicidin in SDS micelles (1g8c.pdb).

structures differed from the linear forms seen in SDS micelles (2,3,9), and are more consistent with structures deduced from circular dichroism spectroscopy studies of indolicidin interacting with palmitoyl-oleoyl-phosphatidylcholine and palmitoyl-oleyoyl-phosphatidylglycerol vesicles (4).

From our simulations, the backbone root mean-square deviation of indolicidin was ~0.55 Å in zwitterionic bilayers (DSPC, 0.55 Å; DOPC, 0.56 Å), and ~0.66 Å in anionic bilayers (DSPG, 0.65 Å; DOPG, 0.67 Å). A similar trend in root mean-square deviation values was seen for the peptide side chains. These data are quite comparable to those reported in the previous NMR study (3). We also found that the backbone root mean-square fluctuation profile (data not shown) was similar to that reported in Khandelia and Kaznessis (9). We noted that the root mean-square fluctuation for the membrane-bound peptide was larger for the anionic bilayers compared to the zwitterionic cases (Fig. 1 *C*).

Not unexpectedly, our simulations revealed that the number of peptide-lipid hydrogen bonds increased with decreasing indolicidin-membrane separation. Specifically, persistent bonds formed between backbone amides of I1, L2, R12, and R13, and the side-chain amines of K5, R12, and R13, with either the phosphate or glycerol oxygens of the lipid headgroups. Although no backbone hydrogen bonds were found in the peptide when it was bound to zwitterionic bilayers, similar to what has been reported in indolicidin-detergent interactions (3,9), we did find backbone hydrogen bonds formed between W4-W6, W6-W9, and/or W9-W11 when it interacted with an anionic bilayer. It has been suggested that the formation of a more ordered secondary structure upon binding with a membrane significantly reduces the energy cost of partitioning a peptide into the interface region (11). Aside from the obvious charge-charge attraction, this observation may provide another basis for the enhanced association of indolicidin with anionic membranes.

Indolicidin's preference for the lipid-water interfacial region has been attributed to its high tryptophan content with the bulky and partially charged indole side group readily accommodated by the electrostatic heterogeneity in this region (12). In Fig. 2, the average insertion depths of the five indolicidin tryptophan residues are shown where zero refers to the center-of-mass of the phosphorus atom of the lipid headgroups. With the exception of DSPC, for all the lipid compositions examined here, W8 penetrated the furthest, followed by W4, to the depth of glycerol oxygens of the lipid headgroups.

In our previous combined AFM-confocal microscopy study of indolicidin binding to phase-segregated supported planar lipid bilayers, we observed an ~1.5-nm lowering of the fluid phase domains upon indolicidin binding (7). In our computational studies, a similar effect was noted. To quantify this, we first defined peptide-associated lipid molecules to be those found within 1.5 nm of the peptide backbone. The extent of membrane thinning was then determined by taking the difference between bilayer thicknesses of the associated and nonassociated lipids, with the largest effect (~4.1 Å) seen in the DOPG bilayers. We note that the differences between our simulated and experimental data may be due to the extent of indolicidin association with the membrane bilayers. In the case of the simulations, we were only considering isolated peptides whereas in the real-world experiments, it is likely that there are cooperative effects between indolicidin molecules during membrane binding. Data obtained from peptide-free bilayer simulations revealed that the bilayer thicknesses fluctuated ~0.033 nm over the same timescale, suggesting that the changes in the bilayer thickness seen in the presence of the peptide are indeed due to indolicidin binding.

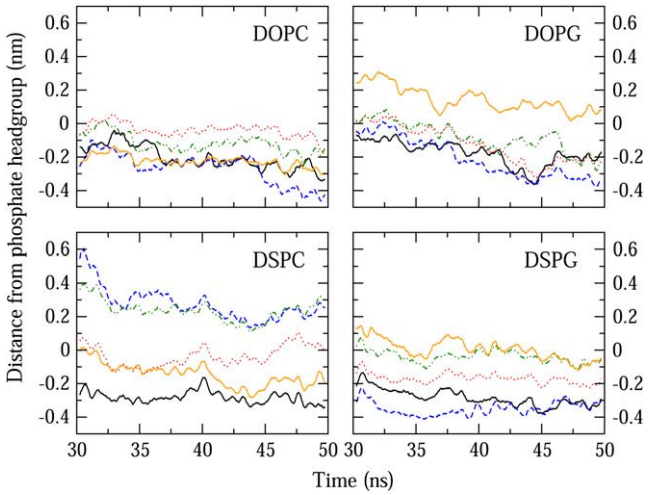

FIGURE 2 Running averages of the distance between the center-of-mass of tryptophan residues and phosphorus atoms of top bilayer leaflet over the last 20 ns of the simulations; W4 (*black solid*), W6 (*red dot*), W8 (*blue dash*), W9 (*green dot dash*), W11 (*orange solid*). A more negative value corresponds to deeper penetration into the bilayer.

It is possible that the observed reduction in membrane thickness was due to interdigitation of the lipid molecules and/or disordering of the upper bilayer leaflet during peptide binding (13–15). Indeed close inspection of the simulation data revealed that both mechanisms were present. As can be seen in Fig. 3, interdigitation of lipid tails for the peptide-associated lipids does occur, along with local disorder of the membrane. We have quantified this disorder by examining the changes in the deuterium order parameters (16), $S_{CD} = \langle 1/2\ (3\cos^2\theta - 1)\rangle$, for the associated and nonassociated lipid carbon tails. In our anionic bilayer simulations, the associated lipid molecules had a much lower S_{CD} value for those carbon atoms situated just below the headgroups, corresponding to a lower degree of orientational order, compared with the nonassociated lipids. In simulations with zwitterionic bilayers, there was no discernable trend in the S_{CD} values for either of the associated or nonassociated lipids. We also noted that the radial distribution of lipid phosphorus atoms located ~4 Å from the peptide was significantly higher after the peptide has fully associated with the bilayer than at the beginning of the simulation. These data strongly support a model wherein as indolicidin partitions into the membrane interface, it recruits surrounding lipids, leading to a local disruption of headgroup packing and leaflet interdigitation for the peptide-associated lipids. The net result is localized thinning of the membrane for the peptide-associated regions.

In agreement with our previously reported AFM studies, our computational simulations of indolicidin binding to model-supported lipid bilayers have revealed atomistic details of lipid disordering upon peptide association. Our data suggest that although electrostatic interactions play a role in the initial peptide-membrane attraction, interfacial partitioning of the peptide is largely driven by sequence hydrophobicity, as has been suggested by several studies of indolicidin analogs (5,17). Computational simulations of indolicidin analogs are underway to provide additional insights to these putative membrane disruption mechanisms.

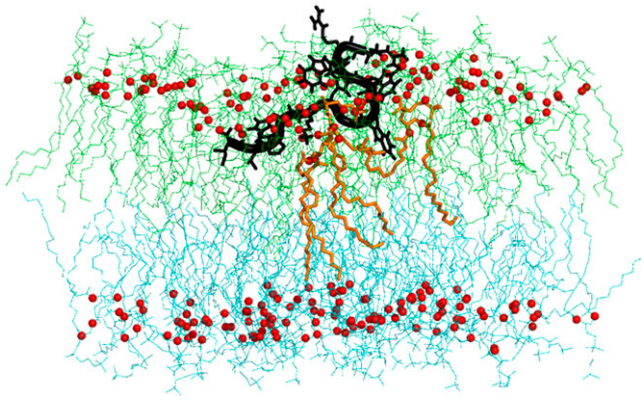

FIGURE 3 A snapshot of lipid tail interdigitation in DOPC; *t* = 43 ns. Upper leaflet is colored in lime and the lower leaflet is colored in cyan. Glycerol oxygens of the phospholipids are drawn as red spheres. The tails of two lipid molecules (*orange sticks*) penetrate into the lower leaflet as their headgroups interact with indolicidin (*black tube*).

ACKNOWLEDGMENTS

This work was supported by Canadian Institutes of Health Research and the Canada Research Chairs program (C.M.Y.). J.H. thanks Canadian Institutes of Health Research and Ontario Graduate Scholarship Program for scholarship support.

REFERENCES and FOOTNOTES

1. Osapay, K., D. Tran, A. S. Ladokhin, S. H. White, A. H. Henschen, and M. E. Selsted. 2000. Formation and characterization of a single Trp-Trp cross-link in indolicidin that confers protease stability without altering antimicrobial activity. *J. Biol. Chem.* 275:12017–12022.
2. Hsu, C. H., C. Chen, M. L. Jou, A. Y. Lee, Y. C. Lin, Y. P. Yu, W. T. Huang, and S. H. Wu. 2005. Structural and DNA-binding studies on the bovine antimicrobial peptide, indolicidin: evidence for multiple conformations involved in binding to membranes and DNA. *Nucleic Acids Res.* 33:4053–4064.
3. Rozek, A., C. L. Friedrich, and R. E. Hancock. 2000. Structure of the bovine antimicrobial peptide indolicidin bound to dodecylphosphocholine and sodium dodecyl sulfate micelles. *Biochemistry.* 39:15765–15774.
4. Schibli, D. J., R. F. Epand, H. J. Vogel, and R. M. Epand. 2002. Tryptophan-rich antimicrobial peptides: comparative properties and membrane interactions. *Biochem. Cell Biol.* 80:667–677.
5. Subbalakshmi, C., V. Krishnakumari, R. Nagaraj, and N. Sitaram. 1996. Requirements for antibacterial and hemolytic activities in the bovine neutrophil derived 13-residue peptide indolicidin. *FEBS Lett.* 395:48–52.
6. Subbalakshmi, C., and N. Sitaram. 1998. Mechanism of antimicrobial action of indolicidin. *FEMS Microbiol. Lett.* 160:91–96.
7. Shaw, J. E., J. R. Alattia, J. E. Verity, G. G. Prive, and C. M. Yip. 2006. Mechanisms of antimicrobial peptide action: studies of indolicidin assembly at model membrane interfaces by in situ atomic force microscopy. *J. Struct. Biol.* 154:42–58.
8. van der Spoel, D., E. Lindahl, B. Hess, G. Groenhof, A. E. Mark, and H. J. Berendsen. 2005. GROMACS: fast, flexible, and free. *J. Comput. Chem.* 26:1701–1718.
9. Khandelia, H., and Y. N. Kaznessis. 2007. Cation-pi interactions stabilize the structure of the antimicrobial peptide indolicidin near membranes: molecular dynamics simulations. *J. Phys. Chem. B.* 111:242–250.
10. Ladokhin, A. S., M. E. Selsted, and S. H. White. 1997. Bilayer interactions of indolicidin, a small antimicrobial peptide rich in tryptophan, proline, and basic amino acids. *Biophys. J.* 72:794–805.
11. Ladokhin, A. S., and S. H. White. 2001. Protein chemistry at membrane interfaces: non-additivity of electrostatic and hydrophobic interactions. *J. Mol. Biol.* 309:543–552.
12. Yau, W. M., W. C. Wimley, K. Gawrisch, and S. H. White. 1998. The preference of tryptophan for membrane interfaces. *Biochemistry.* 37: 14713–14718.
13. Jang, H., B. Ma, T. B. Woolf, and R. Nussinov. 2006. Interaction of protegrin-1 with lipid bilayers: membrane thinning effect. *Biophys. J.* 91:2848–2859.
14. Ludtke, S., K. He, and H. Huang. 1995. Membrane thinning caused by magainin 2. *Biochemistry.* 34:16764–16769.
15. Mecke, A., D. K. Lee, A. Ramamoorthy, B. G. Orr, and M. M. Banaszak Holl. 2005. Membrane thinning due to antimicrobial peptide binding: an atomic force microscopy study of MSI-78 in lipid bilayers. *Biophys. J.* 89:4043–4050.
16. Seelig, J. 1977. Deuterium magnetic resonance: theory and application to lipid membranes. *Q. Rev. Biophys.* 10:353–418.
17. Staubitz, P., A. Peschel, W. F. Nieuwenhuizen, M. Otto, F. Gotz, G. Jung, and R. W. Jack. 2001. Structure-function relationships in the tryptophan-rich, antimicrobial peptide indolicidin. *J. Pept. Sci.* 7:552–564.